Climate Dynamics
https://doi.org/10.1007/s00382-024-07389-7

ORIGINAL ARTICLE

On the present and future changes in Indian summer monsoon precipitation characteristics under different SSP scenarios from CMIP6 models

Marc Norgate[1,2] · **P. R. Tiwari**[1,2] · **Sushant Das**[3] · **D. Kumar**[4]

Received: 13 May 2024 / Accepted: 2 August 2024

Abstract

Monsoons are a vital part of the agriculture and economy of India which most of its population rely on for their livelihoods. It still is not clear how climate change will impact precipitation events over India due to the complexity of accurately modelling precipitation. Using twelve Coupled Model Intercomparison Project Six (CMIP6) models, we compared their performance to observed data taken from CRU as well as looking at the future changes in precipitation until the end of the twenty first century for the **six** precipitation homogenous regions over India. The individual models showed varying degrees of wet and dry biases and the ensemble mean of these models showed relatively lesser bias and improved spatial correlation. Out of 12 models, NorESM and MIROC6 models outperform other models in terms of capturing the spatial variability of precipitation over the Indian region. It is also found that due to lesser moisture transport from the adjoining seas represented through vertically integrated moisture transport (VIMT) analysis, there is consistent dry bias across the models. Further a comprehensive analysis of model performance across six homogeneous precipitation regions indicates that NorESM demonstrates better performance in the CNE and HR regions, EC-Earth excels in the PR, WC, and NE regions, while CMCC shows better performance specifically in the NW region compared to other models. Shared Socioeconomic Pathways (SSPs) were used for future projections and a slight increase in June, July, August, and September (JJAS) precipitation until the end of the century with SSP5-8.5 showing the largest increase. We found an increase in precipitation of 0.49, 0.74 and 1.4 mm/day under SSP1-2.6, SSP2-4.5 and SSP5-8.5 in the far future. The northeast region was shown to receive the largest increase in precipitation (2.9 mm/day) compared to other precipitation homogenous regions and northwest will experience largest shift in precipitation. Interestingly, the number of wet days is expected to increase in the northwest region implying more VIMT towards the region. Our results indicate that monsoon precipitation extremes across all the homogenous regions will increase into the future with a higher severity under fossil-fuelled development, although the models still show large biases lowering confidence in our results.

Keywords Climate change · Indian monsoon · CMIP6 · Future projections

1 Introduction

Monsoons affect two thirds of the world's population and are essential for sustainable agriculture and economic development, with a larger impact on lesser developed countries (Zhou et al. 2016). Agriculture in India relies on the Indian summer monsoon (ISM) and is an important part of the Indian economy, which many people rely on for their livelihood (Krishna Kumar et al. 2004). Rice is one of the main crops grown in the region and is highly susceptible to changes in rainfall (DeFries et al. 2016). Changes to the amount of rainfall can have a damaging effect on the population, with too much or too little rainfall leading to

✉ P. R. Tiwari
p.r.tiwari@herts.ac.uk

1 Centre for Atmospheric and Climate Physics Research, University of Hertfordshire, Hatfield, UK

2 Centre for Climate Change Research, University of Hertfordshire, Hatfield, UK

3 Department of Earth and Atmospheric Sciences, National Institute of Technology Rourkela, Rourkela, Odisha, India

4 Department of Meteorology, University of Reading, Reading, UK

Published online: 14 October 2024

events such as flooding, landslides, droughts and crop failure (Webster et al. 1998). Historically, it has been shown that global monsoon land precipitation has been decreasing, with the South Asian monsoon being one of the primary causes (Zhou et al. 2008). There has been an increase in extreme precipitation over most of India in the past 120 years, with urbanisation correlating to an increase in the intensity of these extreme events (Falga and Wang 2022).

The ISM falls between June, July, August, September (JJAS) and provides about 80% of the total annual rainfall over India (Kripalani et al. 2003). There are many factors that can affect the ISM such as the topography of the region (Medina et al. 2010) and soil moisture (Asharaf et al. 2012) making it a very complex system to model and understand. Several modelling studies confirmed that orography representation governs spatial distribution of precipitation over India (Song et al. 2009; Sinha et al. 2013; Tiwari et al. 2017) by providing a detailed description about the thermal and dynamical effects of the orography. These studies demonstrated that increased/decreased orography in the model correlates with increase/decrease Indian Monsoon precipitation and hence clearly indicates that the model's ability to correctly represent the Himalayas has a significant impact on precipitation results. The Asian Monsoon shows a higher sensitivity to global warming when compared to other monsoon domains (Kitoh et al. 2013) meaning an increase in greenhouse gas (GHG) emissions could lead to a more intense ISM in the future. Various studies have been conducted reflecting monsoon rainfall and its simulation over South Asia and India (Almazroui et al. 2020; Asharaf and Ahrens 2015; Katzenberger et al. 2021; Menon et al. 2013; Sharmila et al. 2015). Global and regional climate models have been used to look at future changes in precipitation over India until the end of the century with a general agreement that precipitation will increase during this time period. Although models are improving there are large biases between models when simulating precipitation (Gusain et al. 2020; Maharana et al. 2021).

The Coupled Model Intercomparison Project (CMIP) models are global climate models (GCMs) created by modelling groups around the world and are useful tools for assessing changes in past, present and future climate. CMIP models have received various improvements over the years with CMIP6 (Eyring et al. 2016) being the newest iteration of these models. CMIP5 and CMIP6 models have been used in the latest IPCC AR6 report (IPCC 2022) when looking at past and future climate. In CMIP models, the bigger challenges are to simulate precipitation at a regional to local scale accurately. They struggle to accurately represent processes such as clouds which occur on a smaller scale than the GCMs resolutions, which in turn lead to larger uncertainties between models (IPCC 2014). CMIP6 models have been shown to better represent clouds and water vapour over tropical oceans (Jiang et al. 2021) although precipitation biases still exist in CMIP6, with a larger overestimation over higher altitudes (Lun et al. 2021). Another addition to CMIP6 is the inclusion of Shared Socio-economic Pathways (SSPs, Riahi et al. 2017) compared to the Representative Concentration Pathways (RCPs, Moss et al. 2010) used in CMIP5. SSPs represent future changes by considering different future emissions and societal changes for five different future scenarios. Recent studies have demonstrated that CMIP6 provides significant improvements over CMIP5 in simulating the Indian Summer Monsoon (ISM), particularly in reducing model biases in precipitation (Dutta et al. 2022; Gusain et al. 2020; Yu et al. 2024). Despite these advancements, still biases persist among CMIP6 models in their precipitation simulations. (Gusain et al. 2020).

Almazroui et al. (2020) shows that annual mean precipitation is projected to increase into the future, with a greater increase under SSP5-8.5, although there is a relatively large uncertainty due to variations between models. The warming of the Indian Ocean is a likely cause for increased precipitation over India (Turner 2022). It is difficult to assess how much of the projected increase in precipitation is due to anthropogenic factors and not natural variability (Wang et al. 2013), however later studies generally seem to agree that monsoon rainfall will increase in the future because of a warmer climate caused by GHG emissions (Lau et al. 2013; Menon et al. 2013; Asharaf and Ahrens 2015; Sharmila et al. 2015; Pattnayak et al. 2018). The El Niño-Southern Oscillation (ENSO) has been shown to affect ISM precipitation (Goswami 1998; Yang and Huang 2021; Panda et al. 2016). The warming of sea surface temperature (SST) is known as El Niño which have been linked to reduced monsoon rainfall (Goswami 1998; Rasmusson and Carpenter 1983) and the cooling of SST is known as La Niña which have been linked to increased monsoon rainfall (Mujumdar et al. 2012). However, there are still gaps in our understanding of these relationships. The Indian Ocean Dipole (IOD) occurs on a local scale (Webster et al. 1999) and has been shown to influence the ISM, with a strong IOD leading to a wetter ISM (Ratna et al. 2021).

The aim of this paper is the look at the performance of 12 CMIP6 models in simulating precipitation over the 6 India precipitation homogenous regions and the future changes in precipitation over these regions. Large spatial and temporal variability in precipitation exists over all of India which is why we will also be looking at the 6 precipitation homogenous regions, which have been used to represent rainfall in other studies (Dash et al. 2009). Future changes are shown using the latest SSP scenarios added in CMIP6. In addition

to the changes in precipitation, the dynamics associated are also presented. Section 2 goes over the methodology and data used, Sect. 3 discusses the results for historical and future time periods and Sect. 4 concludes our results.

Table 1 CMIP6 models used in study

Model	Country	Horizontal resolution (lon and lat)	Model vertical levels (km)
CANESM5	Canda	128×64	45
CESM2	USA	360×180	70
CMCC-ESM2	Italy	288×192	30
CNRM-CM6-1	France	362×294	75
EC-Earth3	Europe	360×180	75
GFDL-ESM4	USA	360×180	49
HadGEM3-GC31-LL	UK	192×144	85
INM-CM5-0	Russia	180×120	73
KACE-1–0-G	South Korea	192×144	85
MIROC6	Japan	256×128	81
NorESM2-MM	Norway	192×96	47
UKESM1-0-LL	UK	192×144	85

2 Model, methodology and data used

Precipitation over the India precipitation homogenous regions were modelled using 12 CMIP6 models, the details of these models are shown in Table 1. We tested the performance of 17 models originally, however only 12 were chosen for the analysis due to poor performance and data availability. The 12 models mentioned were all chosen due to their positive correlation with the observed data. The CMIP6 data used in this work can be found from the CMIP6 database website (https://esgf-node.llnl.gov/search/cmip6/). The six-rainfall monsoon homogenous regions have been used in this study (Fig. 1), namely the Northwest (NW), West Central (WC), Central North East (CNE), Peninsular Region (PR), North East (NE) and Himalayan Region (HR).

The observed precipitation data is taken from CRU at a resolution of 0.5°×0.5° which has been used to evaluate the

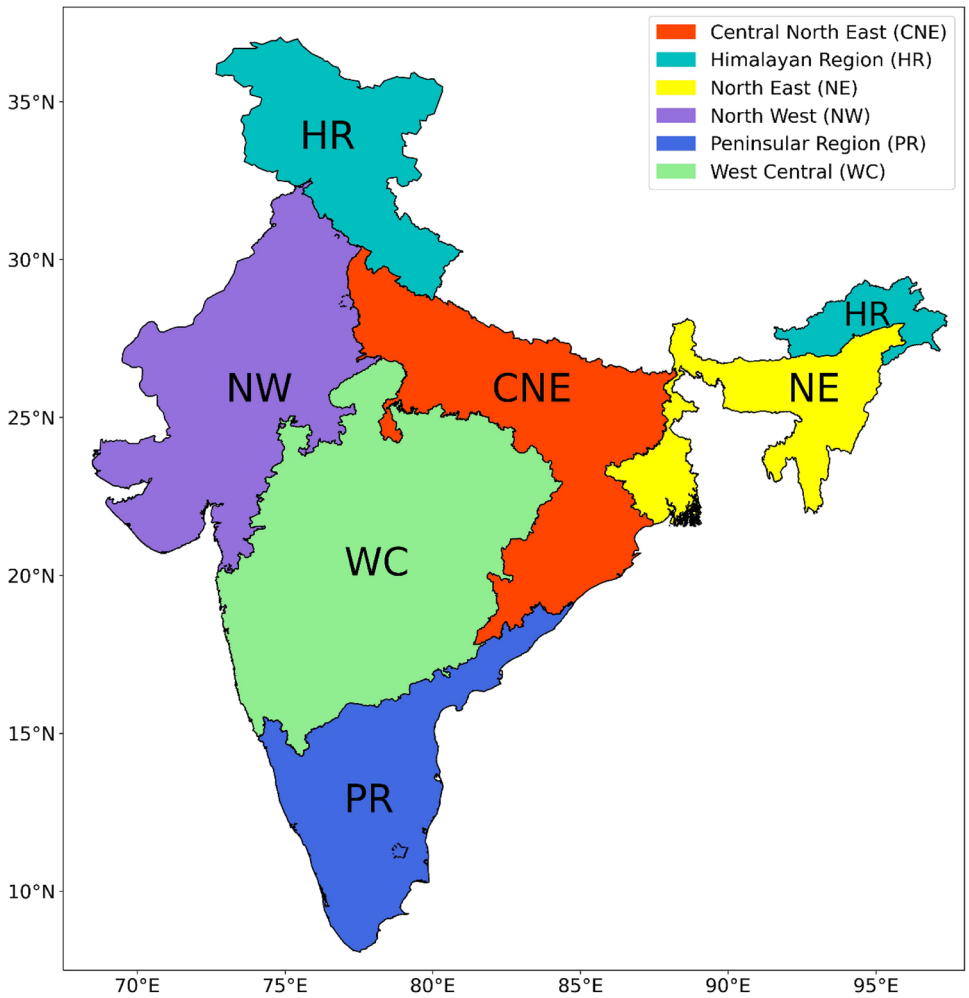

Fig. 1 Six precipitation homogenous regions of India

fidelity of these 12 CMIP6 models. The CRU dataset has been used in many studies and represents precipitation over Indian and South Asian landmass well. ERA5-reanalysis data has been used as the observed dataset when analysing windspeed, humidity and vertically integrated moisture transport over South Asia.

All models have been re-gridded to match the respective observed grid using the bilinear interpolation method with the Climate Data Operator (CDO, Schulzweida 2021) for carrying out the analysis. The historical period is considered from 1984 to 2014 for evaluating all the models. CDO was used to calculate the multi-model mean (MME) for all 12 models to reduce biases from individual models (Evans et al. 2000). The MME is the simple mean of all 12 models in this case.

To test the fidelity of the models the performance of both the individual models and their MME were compared to the observed precipitation. We calculated the difference between the individual models and MME to the observed data during the historical time period to find the biases of the models and MME. Statistical tests have been carried out at 95% significance using the student-t test. Three scenarios i.e., SSP1-2.6, SSP2-4.5 and SSP5-8.5 are considered for investigating future changes in the precipitation characteristics during the Indian summer monsoon season. Briefly the SSP1-2.6 represents a sustainable future, SSP5-8.5 represents fossil-fuelled development and SSP2-4.5 represents a middle road (Riahi et al. 2017). The SSPs used represent low (SSP1-2.6), medium (SSP2-4.5) and high (SSP5-8.5) emission scenarios making SSP5-8.5 the most aggressive scenario in terms of emission. All SSPs represent the future time period 2015–2100 and have been split into near-future (2030–2060) and far-future (2070–2100) to evaluate future changes in precipitation over India. We looked at the projected Indian summer monsoon precipitation for both historical and future time periods. Along with the future changes in the mean precipitation, extreme precipitation indices such as R95, R99, number of consecutive wet days period and wet day index have been examined. The details of the indices are provided in Table 2. Further, diagnosis have been carried out to explain the observed future changes in precipitation from dynamic point of view such as changes in winds at 850 hPa and vertically integrated moisture transport (VIMT).

$$VIMT = -\frac{1}{g}\int_{1000\,\mathrm{hPa}}^{100\,\mathrm{hPa}} (qu + qv)dp,$$

where g is the acceleration due to gravity, q is the specific humidity and u and v are the horizontal and vertical components of the windspeed respectively. The winds at 850 hPa is

Table 2 Extreme precipitation indices definitions calculated using CDO (Schulzweida et al. 2021)

Extremely wet days with reference to the 99th percentile of the reference period	Precipitation percent due to R95p days	Number of consecutive wet days with more than 5 days per time period	Wet days index per time period
The percentage of wet days where the amount of daily precipitation > 99th percentile of the daily precipitation during the historical period	The percentage where daily precipitation amount > the 95th percentile of daily precipitation during the historical period when compared to the sum of the total precipitation	The number of consecutive wet days with ≥ 1mm of daily precipitation that lasts for 5 or more days per JJAS	The number of days where daily precipitation amount is ≥ 1mm

chosen due to its ability to carry the moisture from adjoining seas i.e., Arabian Sea and Bay of Bengal towards the Indian landmass and VIMT calculates the amount of moisture transported from 1000 to 100 hPa.

3 Results and discussion

3.1 Present day monsoon precipitation characteristics

The spatial features of JJAS precipitation over India in the observed data portray a maximum over the Western Ghats, Northeast India, Central and Eastern Indian regions, and Himalayan Foothill regions (Fig. 2a), There is varying success between the models in representing the historical JJAS precipitation climatology over South Asia (Fig. 2). Many of the models can represent these broad spatial features, however a few of them are too dry over the Indian landmass. Although a few of the models do not represent the precipitation hotspots such as the Western Ghats, Himalayan foothills and even the central Indian region, the MME in general outperforms the individual experiments in terms of the spatial distribution. This is also seen in Fig. 3 where we show the biases of the models compared to observations. EC-Earth, HadGEM and NorESM appear to be the best performing models individually and computing the MME of all models shows the best performance. Most models show a dry bias over India, with CanESM5 giving the strongest dry bias (7–9 mm/day) among all the models. The dry bias for JJAS precipitation over India is a known issue with CMIP models, however these biases are shown to improve in CMIP6 compared to CMIP5 (Choudhury et al. 2021; Guilbert et al. 2023). Some models show a large wet bias which is seen mostly over the Himalayan foothills (CESM2, CMCC, MIROC6). The dots in these figures show areas of high confidence which can be seen over the whole region for most figures, except the Northeast of India for the MME and NorESM. The strong dry biases in most of the models affect the MME and major parts of Northern and Northwestern India have dry biases of the order of 3–5 mm/day in them.

Further, we investigate the model performance for the JJAS daily mean precipitation for individual homogeneous regions using the spatial correlation between the models and the observation. Most of the regions of the Indian precipitation homogenous regions (Fig. 1) show a good spatial correlation when comparing the models and MME to

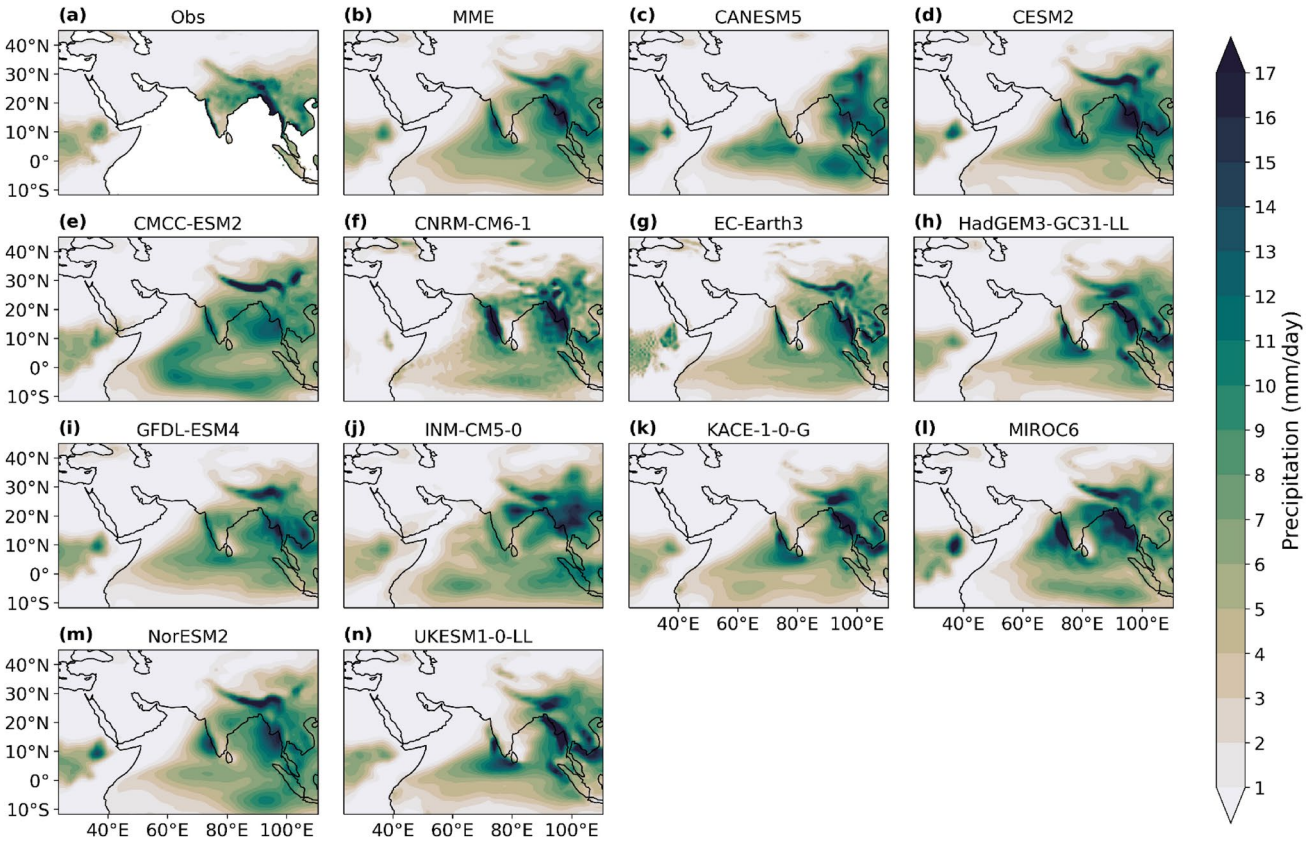

Fig. 2 JJAS precipitation over South Asia (1984–2014) for observed (**a**), MME (**b**) and individual models (**c**–**n**)

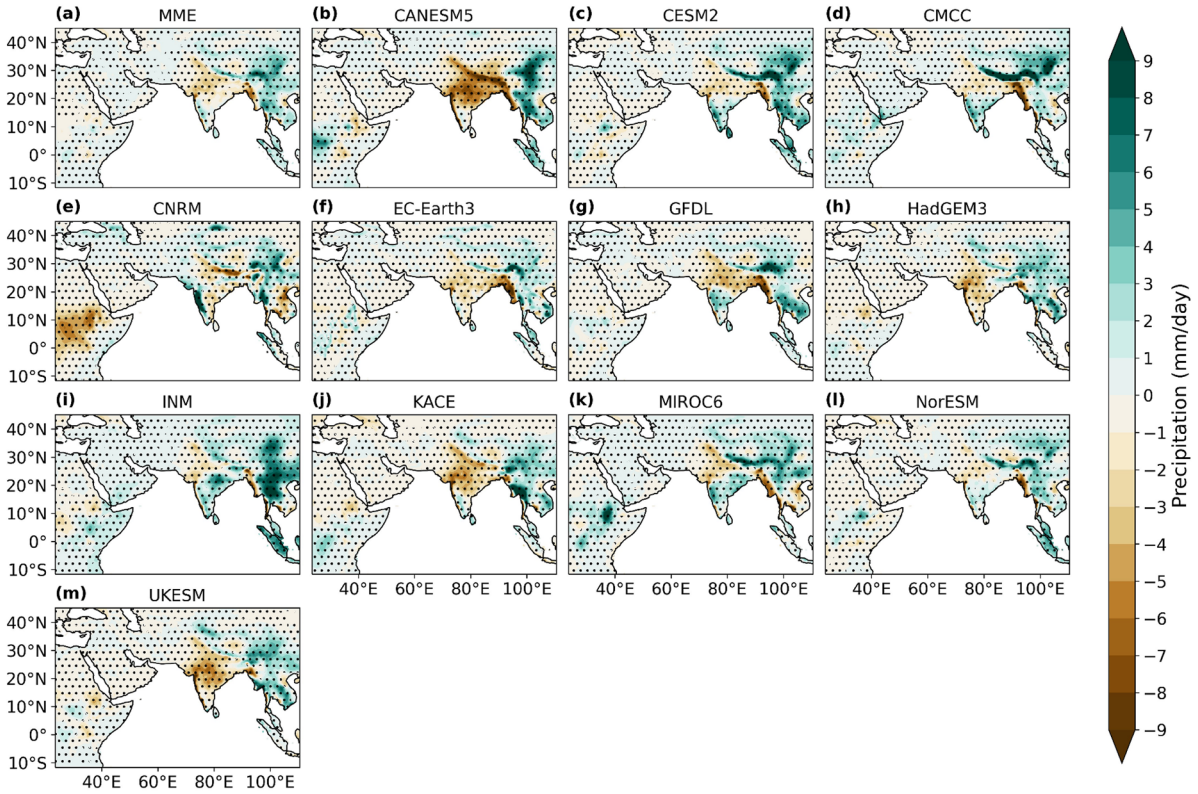

Fig. 3 JJAS precipitation bias over South Asia (1984–2014) for observed (**a**), MME (**b**) and individual models (**c**–**n**). The dots represent the grid points with significant differences at 95% significance level

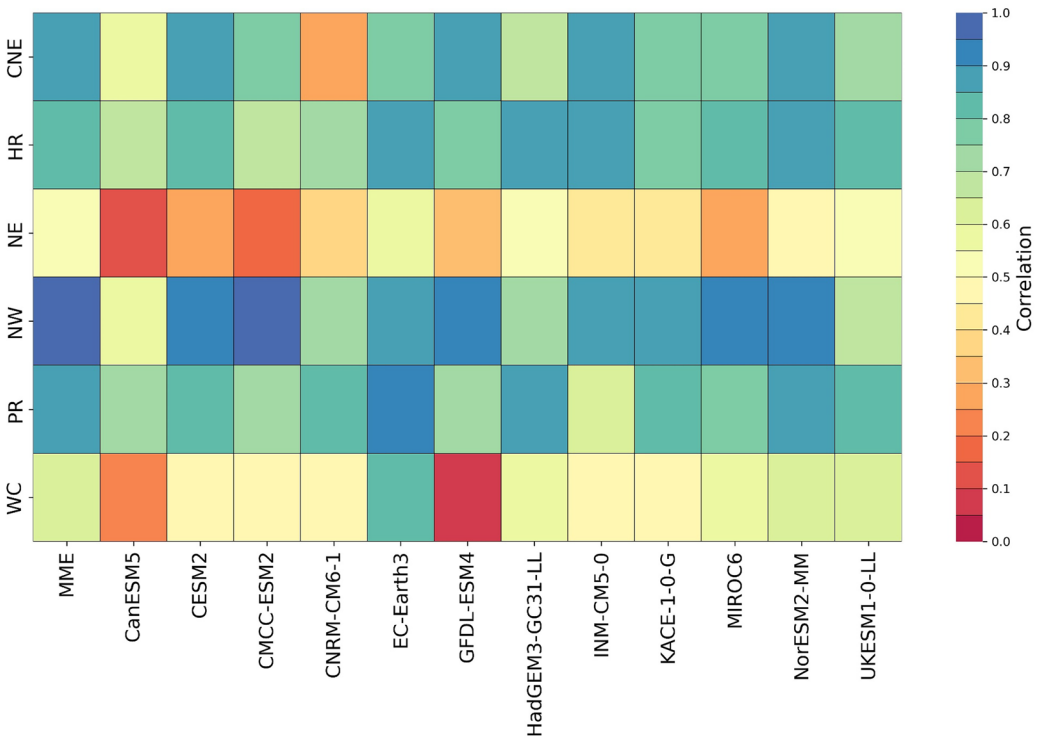

Fig. 4 JJAS precipitation spatial correlation for MME and individual models compared to observed data over each Indian precipitation homogenous region

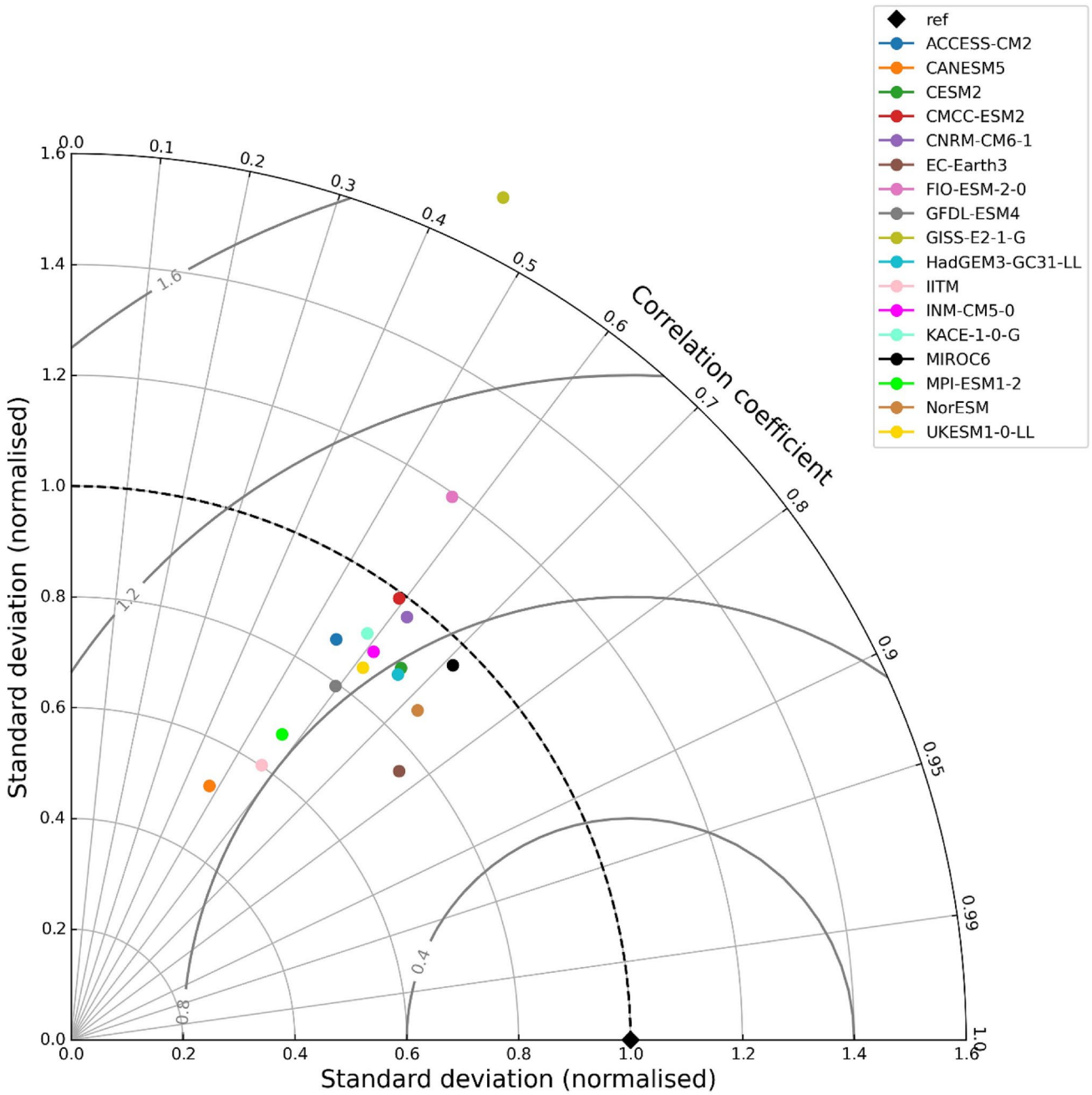

Fig. 5 Taylor diagram for precipitation over India landmass compared to observed data for 17 CMIP6 models

observed values (Fig. 4). Most models show a good correlation over CNE with the highest values being 0.8–0.9. CNRM is much worse over this region compared to other models. The models do well across the board when representing the HR. Over half of the models have a correlation between 0.8 and 0.9. The NE is the worst represented region by all the models where CanESM5 and CMCC give the lowest values of 0.1–0.2. The NW shows the highest correlation between models and observed with the MME, CESM2, CMCC, GFDL, MIROC6 and NorESM performing the best over this region. CanESM5 shows the lowest correlation over this region. The PR is another well represented region by the chosen models. EC-Earth3 has the highest correlation and INM has the lowest. Finally, the WC is poorly represented and GFDL performs the worst over this region, however EC-Earth is the only model that does very well over this region. The MME consistently performs well over all regions when compared to the individual models highlighting the value of the MME. In general, the MME can capture the spatial patterns of precipitation over multiple regions with reasonable

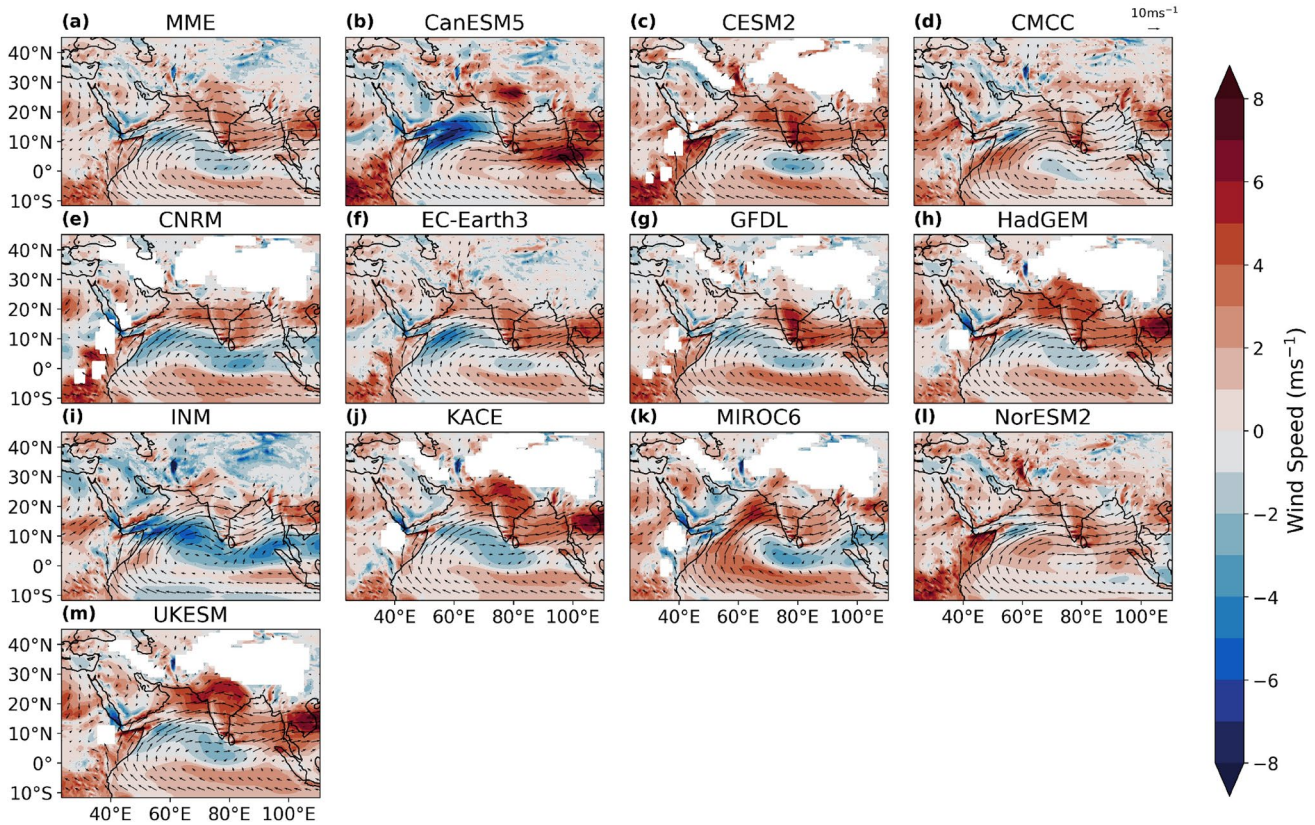

Fig. 6 JJAS windspeed (850 hPa) bias over South Asia (1984–2014) for MME (**a**) and individual models (**b**–**m**) compared to observed values from CRU. Arrows show absolute values

skill, despite the large spatial variability in the precipitation patterns across the country. Moreover, a general pattern of poor correlation over high rainfall regions such as the NE, and larger correlation values over scanty rainfall regions, is prominent across models. It is important to note that, although the long-term correlations appear robust, there may be differences in the correlation values depending on the period and region under consideration. This variability may indicate interannual to decadal-scale variability in the model results, which might be captured differently across models.

We further explore the model's performance in terms of their ability to capture the spatial variability of JJAS precipitation with respect to the observation. Figure 5 illustrates the Taylor diagram comprising of the spatial correlation and normalised standard deviation of the seasonal precipitation. The spatial correlation of seasonal precipitation across the models varies largely with CanESM5 (< 0.4) to EC-Earth3 (0.77) and others lying in this broad range. Comparing the standard deviation across models, the model experiments again show a large range of spatial variability compared to the observation. Overall, the NorESM and MIROC6 models outperform other models in terms of capturing the spatial variability of precipitation over the Indian region.

In terms of simulating dynamic field, we also evaluated spatial distribution of wind at 850 hPa also known as monsoon low level jet. In general, it is one of the semi-permanent features of Indian summer monsoon season. Over South Asia the models generally show a positive bias over most of the region and a negative bias with the south-westerly winds at 850 hPa (Fig. 6). Some models do not show data over the mountainous regions (Fig. 6c, e, g, h, j, k, m) at 850 hPa which is why areas such as the Tibetan Plateau are masked. The direction of the South Asian monsoon is captured by the models with varying biases. Over India all models show a positive windspeed bias and in most cases the south-westerly wind shows the most noticeable negative bias, with CanESM5 showing the most extreme negative bias. The absolute windspeed values can be seen in figure S1. The MME for specific humidity (Fig. S3) shows a mostly negative bias over land and positive bias over the ocean, and the landmass east of India. The absolute specific humidity values can be seen in figure S2. Since moisture transport mechanism is important from the adjoining seas towards Indian landmass during the Indian summer monsoon season, we also checked the vertically integrated moisture transport (VIMT). The models underestimate the larger values of the VIMT which suggests an underestimation of

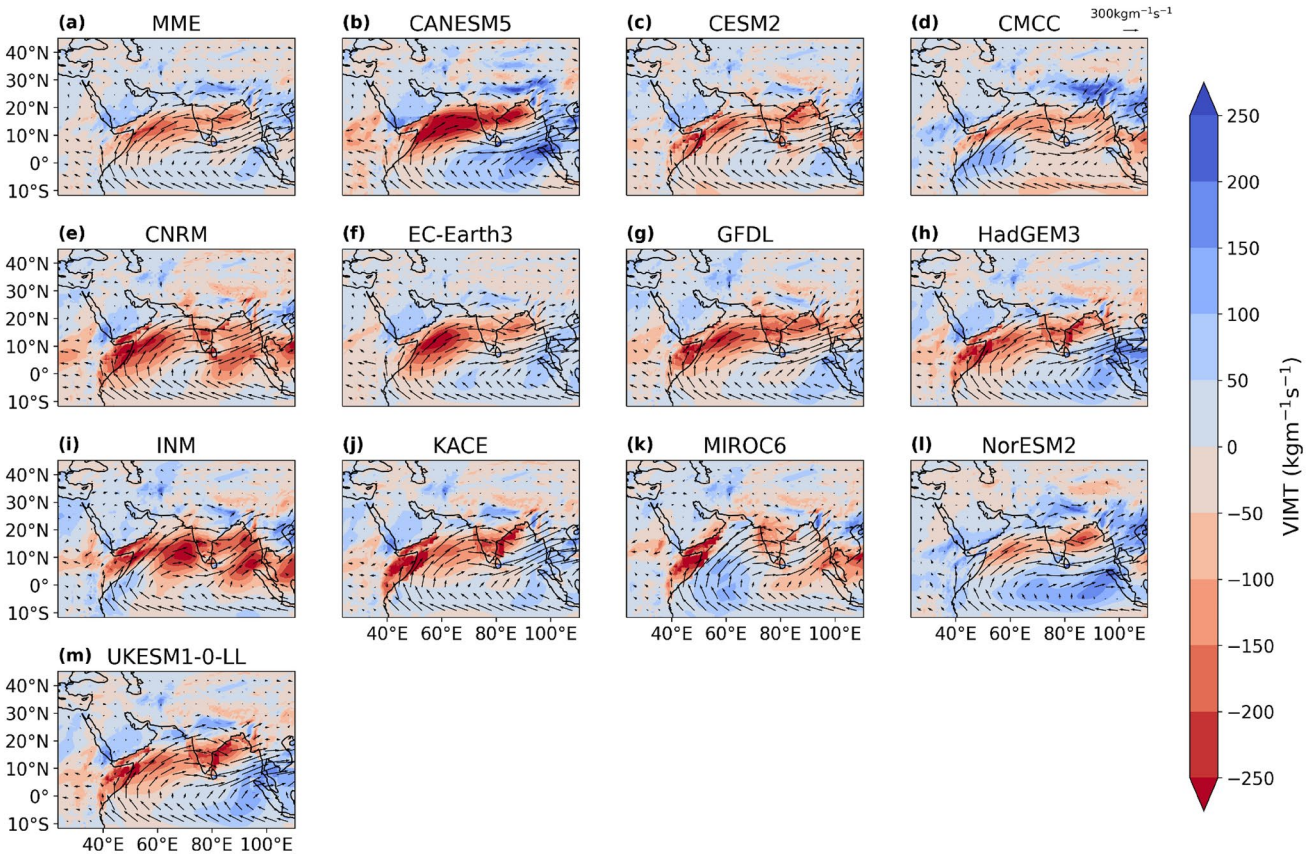

Fig. 7 Vertically integrated moisture transport bias compared to ERA5 for MME (**a**) and individual models (**b**–**m**) over South Asia. The arrows show the absolute values, both bias and absolute values are shown from 1000 to 100 hPa

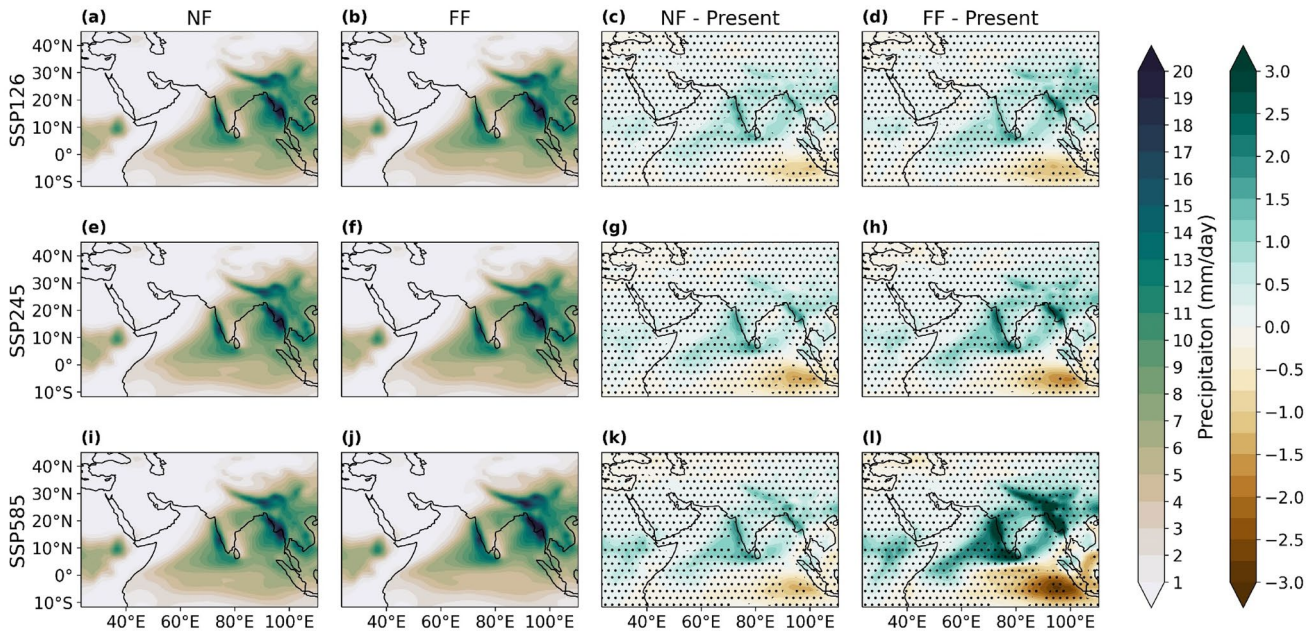

Fig. 8 Mean precipitation difference over South Asia for SSP1-2.6 (**a**, **b**, **c**, **d**), SSP2-4.5 (**e**, **f**, **g**, **h**) and SSP5-8.5 (**I**, **j**, **k**, **l**). The first and second columns show the absolute values for NF (**a**, **e**, **i**) and FF (**b**, **f**, **j**) respectively. The third and fourth columns show the precipitation difference for NF (**c**, **g**, **k**) and FF (**d**, **h**, **l**) respectively when compared to the historical period. The dots represent the grid points with significant differences at 95% significance level

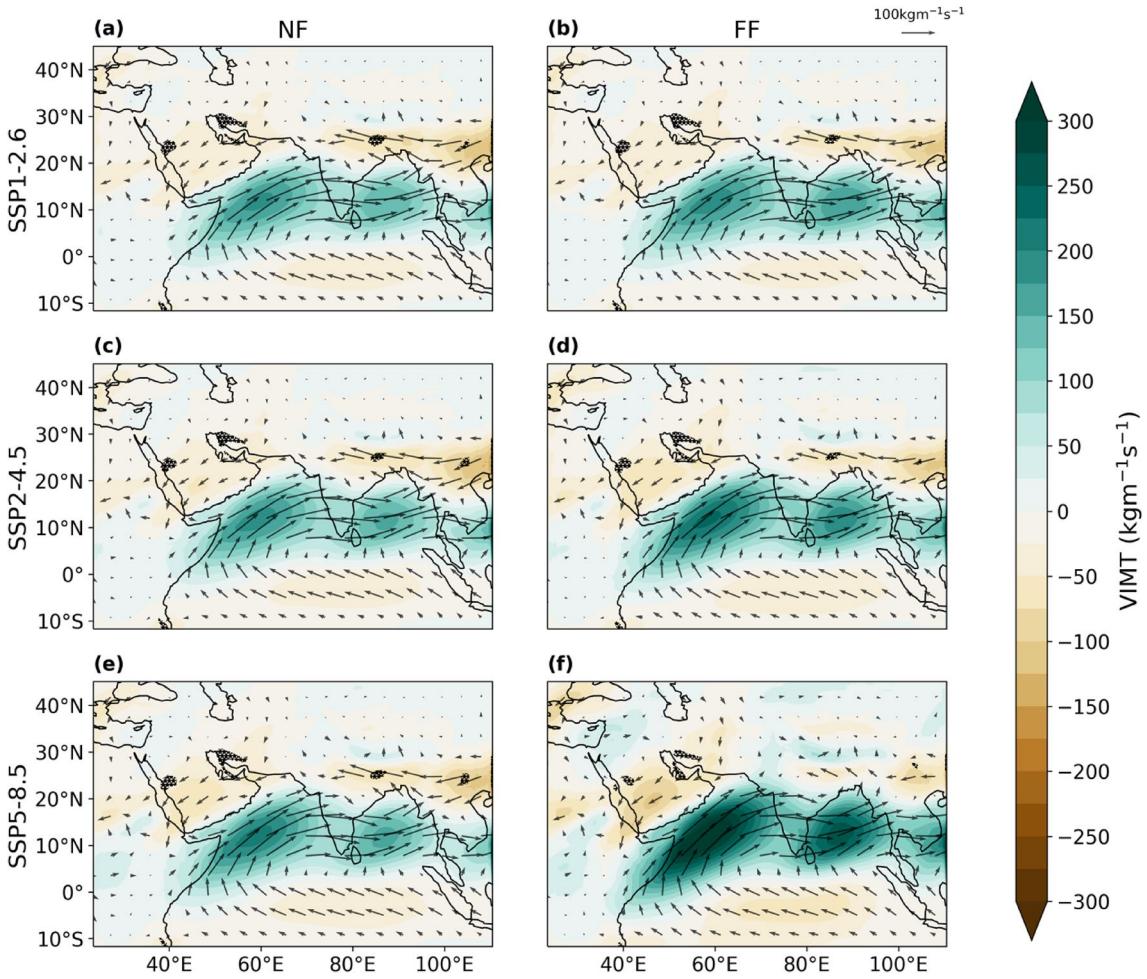

Fig. 9 Vertically integrated moisture transport difference compared to the historical period from 1000 to 100 hPa over South Asia. SSP scenarios SSP1-2.6 (Fig. 12a, b), SSP2-4.5 (Fig. 12c, d) and SSP5-8.5 (**e**, **f**) are used. The SSPs are split into NF (**a**, **c**, **e**) and FF (**b**, **d**, **f**). The dots represent the grid points with significant differences at 95% significance level

monsoon rainfall over this region during the monsoon season (Fig. 7). All models show a negative bias over most of India and a positive bias over the Himalayas. The negative bias over the ocean matches that of the negative bias from the windspeed, although over land VIMT and windspeed biases don't match. The models with a larger negative bias for specific humidity also appear to have a larger negative VIMT bias over India. The negative bias in the VIMT could be the reason for having precipitation dry bias over central part of India. The absolute VIMT values can be seen in figure S4. CanESM5 (Fig. 7b) shows the largest positive and negative biases compared to all other models for VIMT. The most extreme negative bias is to the southwest of India and this is the case for most of the models. MIROC6 (Fig. 7k) is the only model that shows a positive bias over this area. CMCC (Fig. 7d) is the best performing individual model, however there is a relatively large positive bias over northeast India and the surrounding countries comparatively. The MME appears to reduce the magnitude of both positive and negative biases over this region and gives the best VIMT representation overall.

3.2 Future changes in the monsoon precipitation

The spatial changes in the near and far future precipitation during the Indian summer monsoon is shown in Fig. 8. All SSPs show an increase in precipitation in the NF and FF and FF SSP5-8.5 shows the largest increase overall in the South Asian region (Fig. 8). All figures show a very similar coverage in precipitation changes across most of South Asia where most of the precipitation in the region will increase. When comparing the NF SSPs to the present period, there isn't much difference between them. SSP5-8.5 (Fig. 8i, j, k, l) has slightly higher extremes than the other two scenarios. Moving to the FF and the changes are much more dramatic. FF SSP5-8.5 (Fig. 8i) shows the largest increase, with the

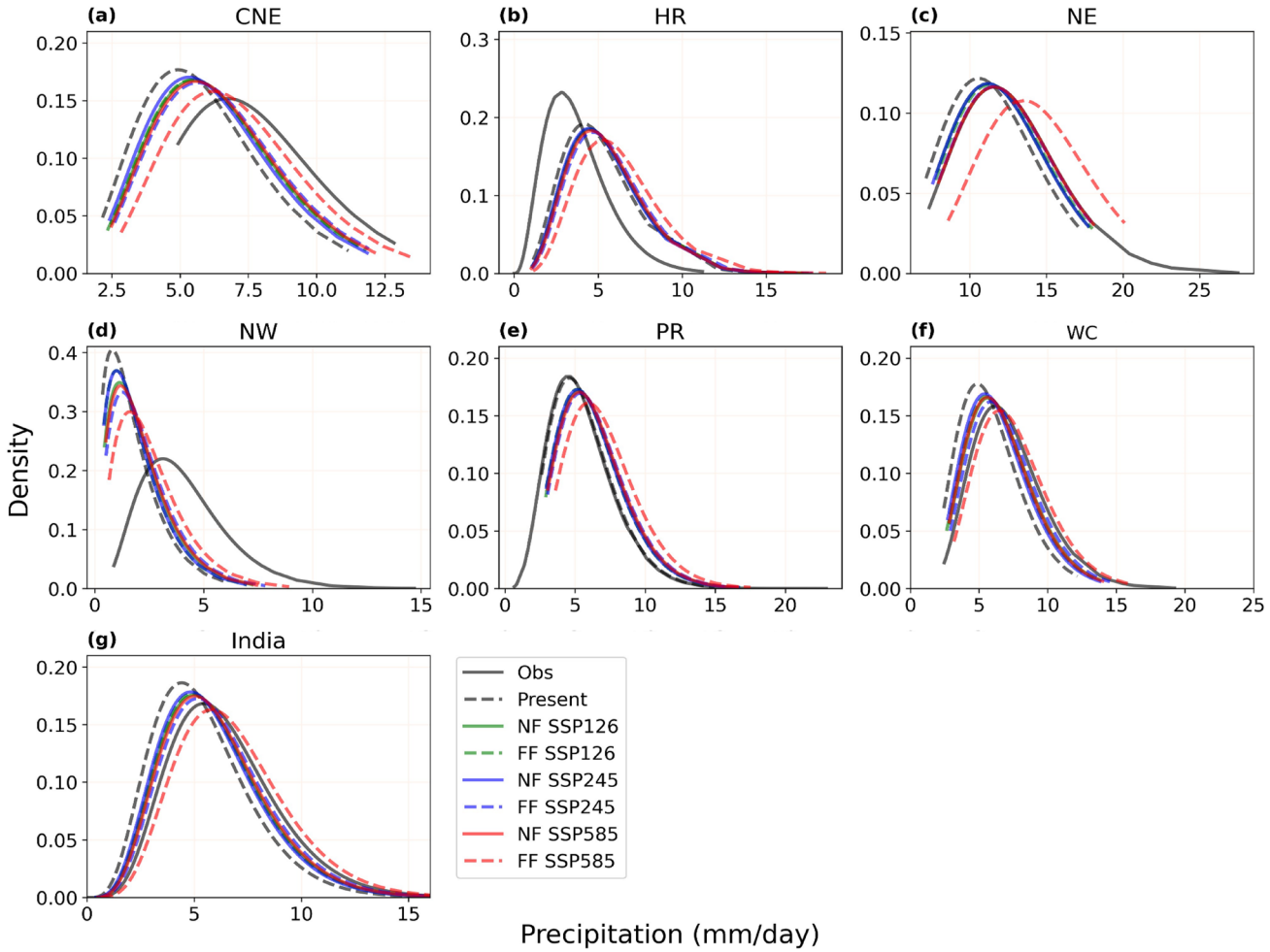

Fig. 10 PDF distribution of precipitation over Indian precipitation homogenous regions (**a**–**f**) and India landmass (**g**). The black lines represent the historical period (1984–2014). The solid and dashed black lines show observed and MME data respectively. For the SSP scenarios green, blue, and red represent SSP126, SSP245 and SSP585 respectively. For the SSPs a solid line shows the NF time period, and a dashed line shows the FF time period

Table 3 Precipitation increase (%) per region compared to historical period (1984–2014)

	CNE	HR	NE	NW	PR	WC
NF_SSP126	9.40	6.53	5.52	18.2	11.6	12.9
NF_SSP245	6.58	5.59	5.33	10.8	10.1	8.94
NF_SSP585	10.6	8.39	8.84	20.9	12.4	12.4
FF_SSP126	9.00	6.94	6.35	10.4	9.77	11.0
FF_SSP245	11.9	10.3	8.59	25.8	13.6	16.9
FF_SSP585	21.4	21.9	25.5	44.6	23.8	27.5

West Coast of India, Bangladesh, Nepal, Bhutan and Myanmar receiving over 3 mm/day more precipitation in the monsoon season. The west coast of India sees most of the South Asian monsoon precipitation, and this increase suggests that the South Asian monsoon will be more extreme in the far future, with the most extreme scenario being FF SSP5-8.5. We have looked into low-level moisture convergence at 850 hPa and found its playing a crucial role in causing more precipitation over the region. This increase in Indian summer monsoon rainfall was also shown by Katzenberger et al. (2021), where all CMIP6 models used in their study as well as the MME showed significant increases in precipitation during FF SSP5-8.5. They also linked this increase in precipitation to an increase in global mean temperature. The

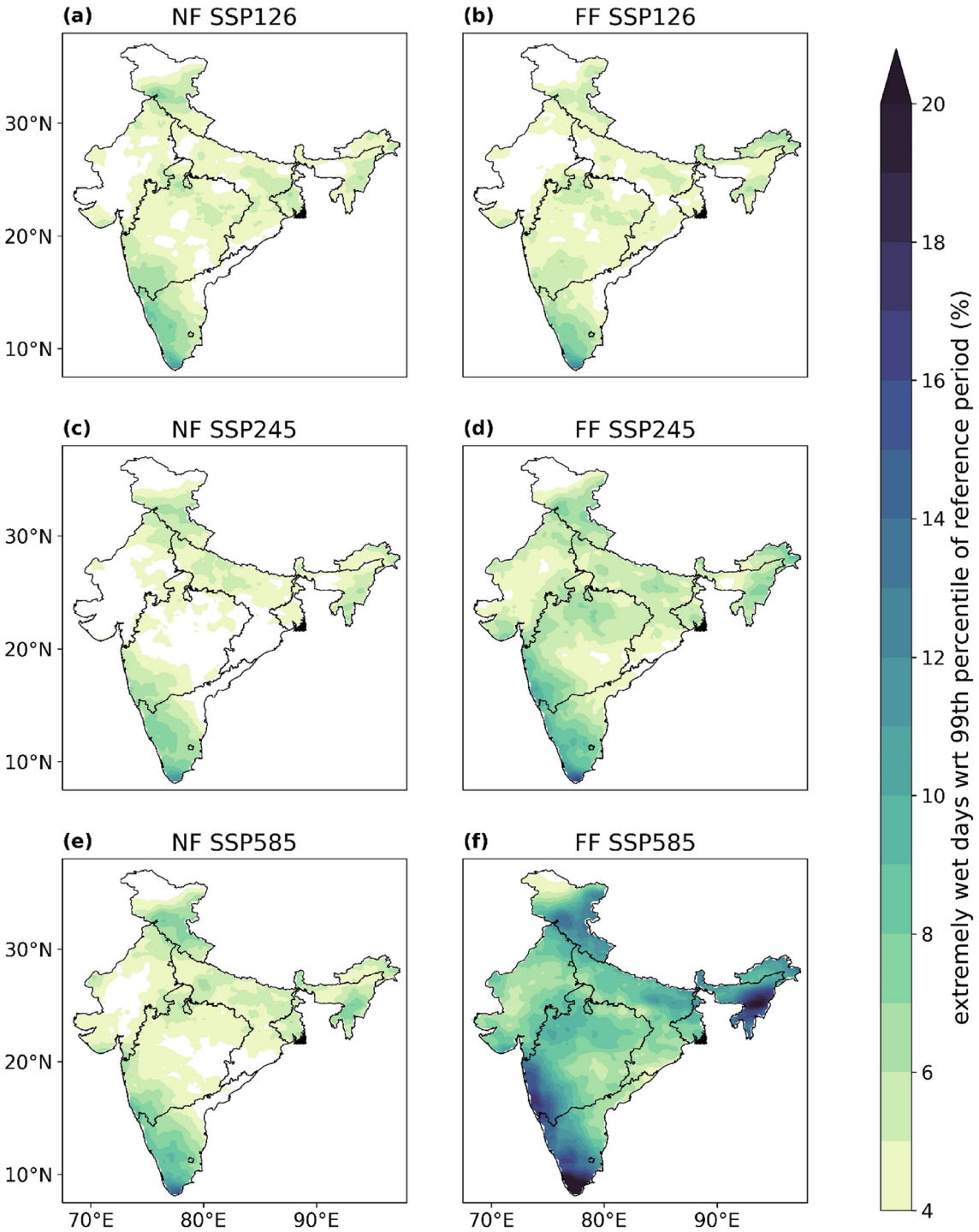

Fig. 11 Extremely wet days with reference to the 99th percentile of reference period (1984–2014). The first column (**a**, **c**, **e**) shows the NF and the second column (**b**, **d**, **f**) shows the FF for SSP126 (**a**, **b**), SSP245 (**c**, **d**) and SSP585 (**e**, **f**)

changes in the VIMT in near and far future under various SSP scenarios are shown in Fig. 9. The FF SSP5-8.5 shows the largest increase in VIMT compared to other SSP scenarios. During the NF (Fig. 9a, c, e) there is little difference between the SSPs. However, in the FF (Fig. 9b, d, f) all SSPs show at least a minor increase in VIMT. The large increase from FF SSP5-8.5 could explain why there is a large increase in precipitation seen in Fig. 8i. An increase in precipitation can be seen over all India precipitation homogenous regions when comparing the present climate to the SSP scenarios

Table 4 Extreme wet days difference (%) per region compared to historical period (1984–2014)

	CNE	HR	NE	NW	PR	WC
NF_SSP126	4.47	4.48	4.67	4.16	5.80	4.72
NF_SSP245	4.23	4.52	4.65	3.86	5.89	4.19
NF_SSP585	4.71	5.13	5.63	4.50	6.75	4.68
FF_SSP126	4.35	4.47	4.63	3.87	5.68	4.68
FF_SSP245	5.21	5.29	5.62	5.14	7.13	5.77
FF_SSP585	7.91	9.40	12.2	7.52	11.6	8.81

using a Gamma distribution (Fig. 10) which has been shown to well represent precipitation data (Wilks 2011). It's important to note that unlike the symmetric Gaussian (Normal) distribution, the Gamma distribution exhibits a pronounced right skewness. This characteristic makes it suitable for modelling daily rainfall, as it accommodates the lower limit of zero which restricts rainfall values (Wilks 2011). The MME for the historical period underpredicts precipitation for all regions (Fig. 10a, c, d, f) as well as the entirety of India (Fig. 10g) except for the PR region (Fig. 10e) which is the best represented and the HR region (Fig. 10b) where the MME overpredicts precipitation. The SSPs over all regions show an increase in precipitation when compared to the historical period and except for FF SSP5-8.5 there is little difference between the NF and FF SSPs. FF SSP5-8.5 shows the largest shift in precipitation for all regions, the largest shift can be seen over the NE region. For the regions CNE, HR, NE, NW, PR, WC and India, FF SSP585 compared to the historical period shows an increase in precipitation of 1.28, 1.12, 2.9, 0.84, 1.36, 1.63 and 1.4 mm/day respectively. FF SSP126 shows an increase of 0.53, 0.03, 0.71, 0.23, 0.56, 0.66 and 0.49 mm/day respectively.

There is an increase in precipitation over all the precipitation homogenous regions of India when comparing NF SSP2-4.5 and SSP5-8.5 to FF SSP2-4.5 and SSP5-8.5 respectively (Table 3). All percentage increases are compared to the historical period. SSP1-2.6 doesn't follow this pattern as over the CNE, NW, PR and WC there is a decrease in percent precipitation when comparing NF to FF. The NW will see the largest increase in precipitation going from 10.8% and 20.9% for NF SSP2-4.5 and SSP5-8.5 respectively to 25.8% and 44.6% for FF SSP2-4.5 and SSP5-8.5 respectively. This means that under SSP5-8.5, the NW will see a 23.7% increase when going from NF to FF as well as the largest increase of 44.6% when compared to the historical period. Comparing NF and FF SSP5-8.5 there is an increase of 10.8%, 13.51%, 16.66%, 23.7%, 11.4% and 15.1% for the CNE, HR, NE, NW, PR and WC respectively.

All SSP scenarios show an increase in extreme wet days (EWD) when compared to the historical period (Fig. 11). During the NF, SSP2-4.5 (Fig. 11c) shows the smallest increase in EWD's, where most of the NW, WC, and the lower half of the CNE regions show no increase at all. NF SSP5-8.5 (Fig. 11e) has the largest increase in EWD compared to the other SSPs, but not by much. The area that sees the largest increase is the southern part of the PR. When comparing NF and FF SSP1-2.6, there is little difference. The NW region sees a slight decrease in EWD. FF SSP2-4.5 shows an increase over all regions except the northern part of the HR. Now all regions show a minimum 4% increase. Under this scenario, the most affected region is the southern PR with a 14% increase. FF SSP5-8.5 shows the largest increase in EWD. All regions will see an increase in EWD with the most affected regions being the west coast of the WC, the west and south coast of the PR and the east of the NE. These regions are showing a $>20\%$ increase in EWD. Table 4 shows the percentage increase in EWD per region when compared to the historical period. There is very little change between NF and FF SSP1-2.6 for all regions and there is an increase in EWD when comparing NF SSP2-4.5 and SSP5-8.5 to FF SSP2-4.5 and SSP5-8.5 respectively. The largest increase for all regions is from FF SSP5-8.5. When comparing the increase from NF to FF for this scenario, we see a 3.2%, 4.27%, 6.57%, 3.02%, 4.85% and 4.13% for the CNE, HR, NE, NW, PR and WC respectively. This means that the NE will receive the largest increase in EWD from both historical and NF to the FF. When going from the historical to the NF, the PR sees the largest increase in EWD of 6.75%.

Similarly, to the previous figure, a much larger increase in precipitation percent due to R95p days can be seen from FF SSP5-8.5 (Fig. 12). All NF SSPs show a similar precipitation percent to each other (Fig. 12a, c, e). There is negligible change between NF and FF SSP1-2.6 (Fig. 12a and b respectively). FF SSP2-4.5 shows an approx. 5% increase which seem to affect the same areas. FF SSP5-8.5 shows a dramatic increase in precipitation percent with the most affected regions increasing by over 40%. The most affected regions are the same as Fig. 11 which are also the regions in India that receive the most rainfall per monsoon season.

Although extreme precipitation has been shown to increase, the consecutive wet days (CWD) do not follow this trend for most regions (Fig. 13). When looking at the NF SSP2-4.5 and SSP5-8.5 show an increase in CWD over the CNE region whereas under SSP1-2.6 this region shows a

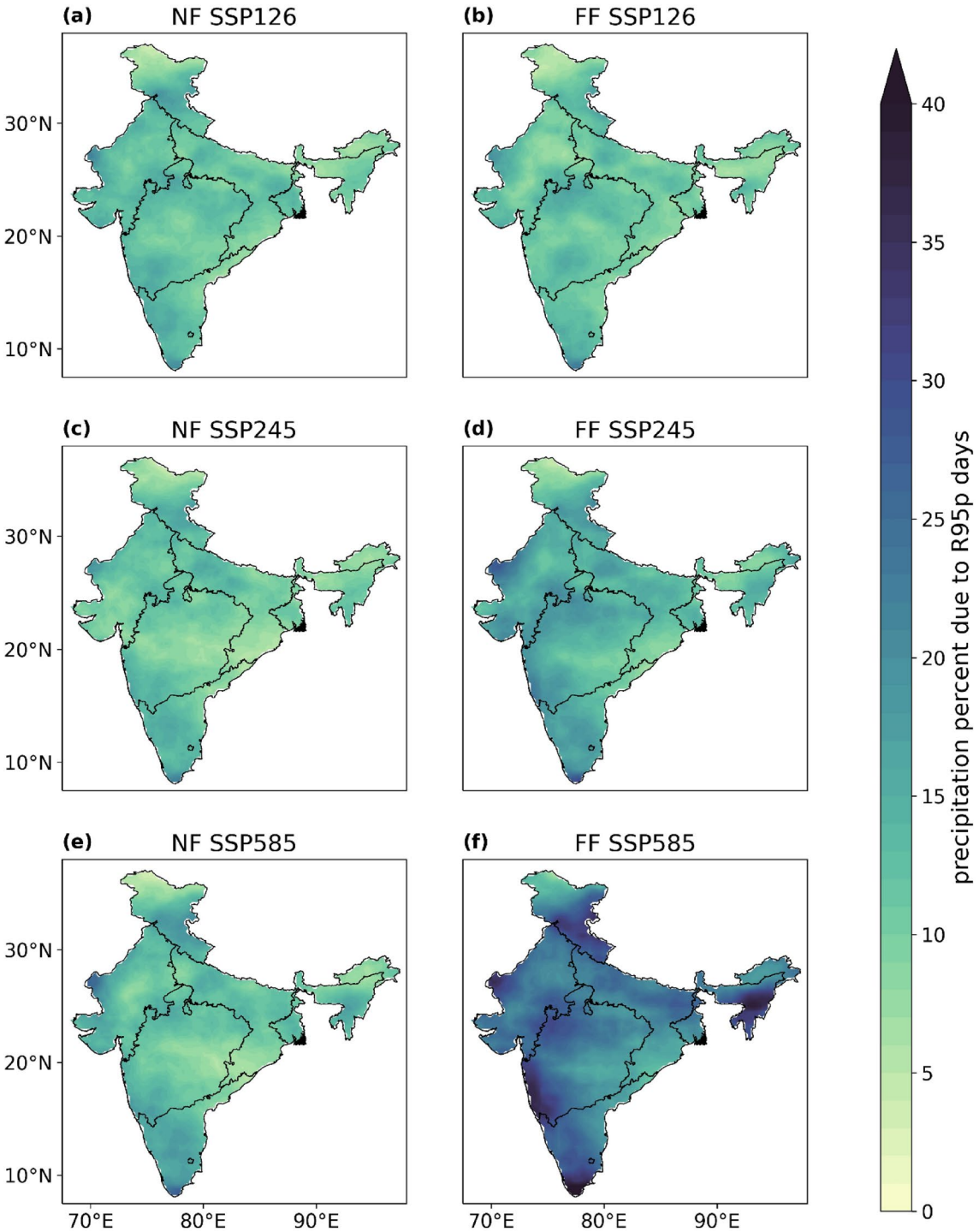

Fig. 12 Precipitation percent due to R95p days. The first column (**a**, **c**, **e**) shows the NF and the second column (**b**, **d**, **f**) shows the FF for SSP126 (**a**, **b**), SSP245 (**c**, **d**) and SSP585 (**e**, **f**)

slight decrease. Most regions show no change or a decrease in CWD, however the NW region shows the largest increase for all SSPs. This could be possible due to larger transport in moisture towards the region as discussed in Fig. 9 NF SSP5-8.5 has more extreme increases and decreases in CWD compared to the other NF SSPs. There is little change between NF and FF SSP1-2.6. FF SSP2-4.5 shows a similar pattern compared to its NF counterpart, but with more extreme values. The CNE however changes from a majority increase in CWD in the NF to a slight decrease by the FF.

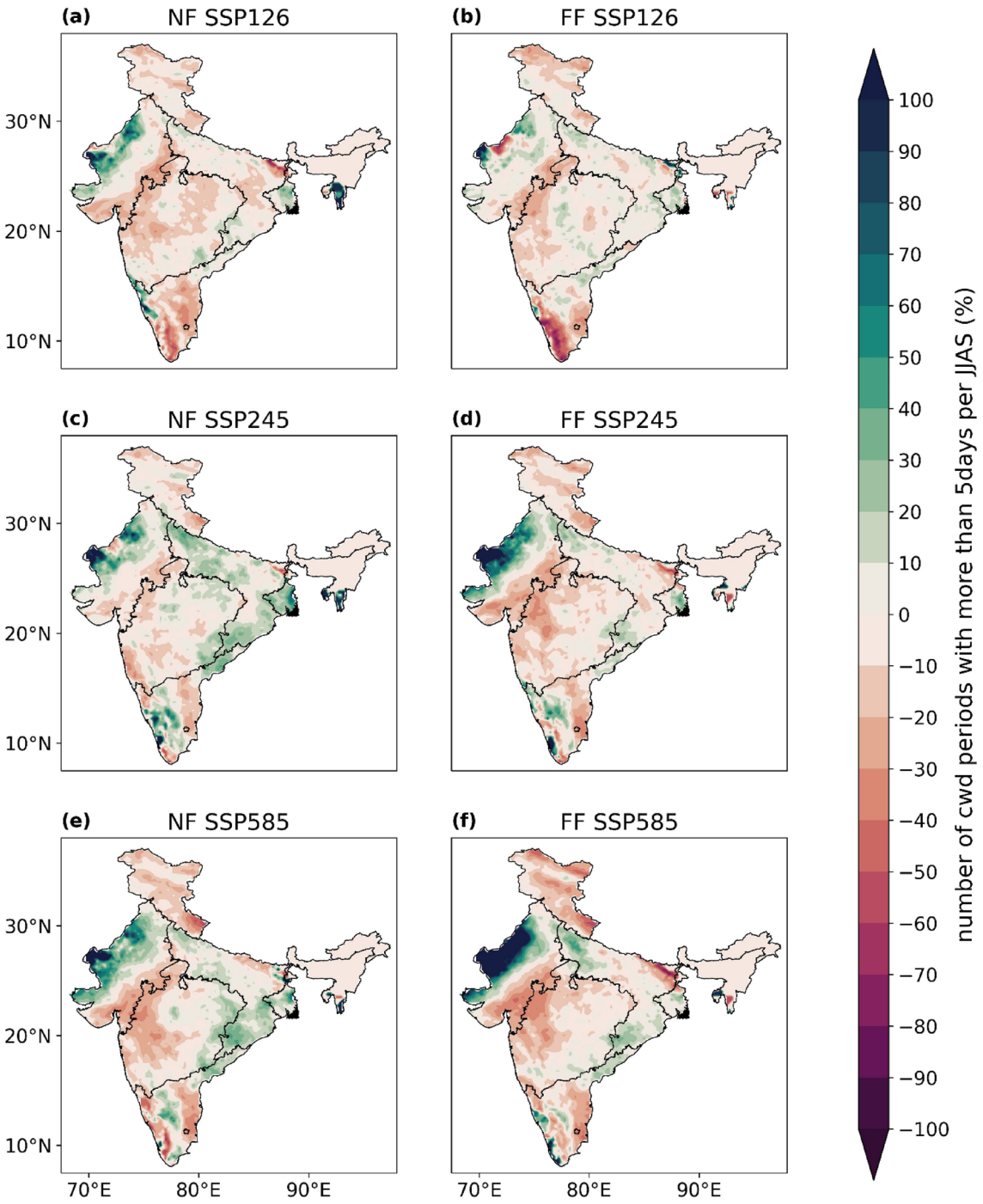

Fig. 13 Percentage difference compared to the historical period for the number of cwd periods with more than 5 days per JJAS season. The first column (**a**, **c**, **e**) shows the NF and the second column (**b**, **d**, **f**) shows the FF for SSP126 (**a**, **b**), SSP245 (**c**, **d**) and SSP585 (**e**, **f**)

The difference between NF and FF SSP5-8.5 shows similar patterns to SSP2-4.5. FF SSP5-8.5 shows the most extreme increases and decreases in CWD. The most affected region appears to be the NW for an increase in CWD. The south-east of NW, east of PR and HR show the largest decrease in CWD.

Small changes in emissions appear to have a very large effect on consecutive dry days (CDD) and consecutive wet days (CWD) which can be seen in Tables 5 and 6 respectively. The CDD decrease when comparing the NF to FF SSP5-8.5 for the CNE, HR, NE and NW and increase for the PR and WC. For CWD the CNE, HR, NE, PR and WC

Table 5 Consecutive dry days difference (%) per region compared to historical period (1984–2014)

	CNE	HR	NE	NW	PR	WC
NF_SSP126	−1.24	−0.814	−55.7	−8.84	−5.99	7.03
NF_SSP245	−2.20	−3.38	57.6	−6.41	35.7	4.56
NF_SSP585	−15.9	−9.32	−3.32	−14.6	−20.0	−5.96
FF_SSP126	8.75	3.81	−47.2	−6.63	4.55	8.24
FF_SSP245	−4.51	6.55	−9.96	−14.3	55.0	12.1
FF_SSP585	−18.6	−17.0	−41.0	−19.8	31.2	13.9

Table 6 Consecutive wet days difference (%) per region compared to historical period (1984–2014)

	CNE	HR	NE	NW	PR	WC
NF_SSP126	−2.97	−8.45	9.97	−3.31	−15.0	−8.73
NF_SSP245	11.5	−5.11	26.4	1.16	−2.69	−2.29
NF_SSP585	7.03	−13.2	12.6	4.17	−8.56	−7.11
FF_SSP126	0.876	−9.80	6.71	−1.46	−9.34	−6.04
FF_SSP245	0.750	−10.2	6.05	1.23	−8.93	−10.4
FF_SSP585	4.32	−18.4	1.65	6.45	−12.6	−10.3

decrease and the NW increases. There is a big difference in CDD over the NE and PR for the different SSPs. For CDD in the PR, from NF SSP1-2.6 to SSP2-4.5 we go from a 5.99% decrease to a 35.7% increase. This is also seen over the NE where we see a 55.7% decrease and then a 57.6% increase for SSP1-2/6 and SSP2-4.5 respectively. This is also seen with CWD for these regions. The NE goes from a 9.97% increase to a 26.4% increase and the PR goes from a 15% decrease to a 2.69% decrease for NF SSP1-2.6 and SSP2-4.5 respectively. This suggests that these regions are highly sensitive to changes in emissions.

The NW region sees a much larger increase in wet days index (WDI) compared to the other regions (Fig. 14). Large scale moisture convergence plays a crucial role in the increase of precipitation over the NW region in near and far future. There is little change in most regions in the NF except the NW, HR and west of the CNE regions. For NF SSP5-8.5 the PR sees more of an increase in WDI compared to the other two SSPs. When comparing NF and FF SSP1-2.6 there is little change and FF SSP1-2.6 shows a slight reduction in WDI overall, with the PR decrease being the most noticeable. For FF SSP2-4.5 and SSP5-8.5 the NW and HR see an increase in WDI and SSP5-8.5 shows a much larger increase in comparison. All FF SSPs show the WDI in the PR decrease and the largest decrease is from FF SSP5-8.5.

Overall, the analysis suggests that out of twelve CMIP6 models NorESM demonstrates better performance in the CNE and HR regions, EC-Earth excels in the PR, WC, and NE regions, while CMCC shows better performance specifically in the NW region compared to other models. This analysis suggests that these specific models can be used for dynamical downscaling over these regions to support robust decision- and policymaking. Further it's also shown that the largest increase in precipitation extreme, is from FF SSP5-8.5. This is comparable to other studies over South Asia who have shown similar results using CMIP5 and CMIP6 models (Dutta et al. 2022; Gusain et al. 2020; Yu et al. 2024).

4 Conclusion

In this study we compare the performance of 12 CMIP6 models in simulating precipitation over South Asia and the precipitation homogenous regions of India. Using the new SSPs implemented in CMIP6, SSP1, 2 and 5 were used to look at future changes in precipitation. The key findings of this study are listed below:

- CMIP6 models demonstrate significant improvement in simulating Indian Summer Monsoon (ISM) precipitation and exhibit reduced model bias in comparison to CMIP5.
- The MME of the models improves the skill when compared to individual models, improving model results as well as reducing the overall biases compared to individual models. There is still a slight dry bias over India and a wet bias to the east of India.
- All SSPs show an increase in precipitation in the future over India with the largest increase from FF SSP5-8.5 of 1.4 mm/day, suggesting that fossil-fuelled development will increase precipitation in the coming century over India. There is a smaller increase in precipitation of 0.49 and 0.74 mm/day under FF SSP1-2.6 and FF SSP2-4.5. The NE region will receive the largest increase in precipitation (2.9 mm/day) compared to other precipitation homogenous regions.

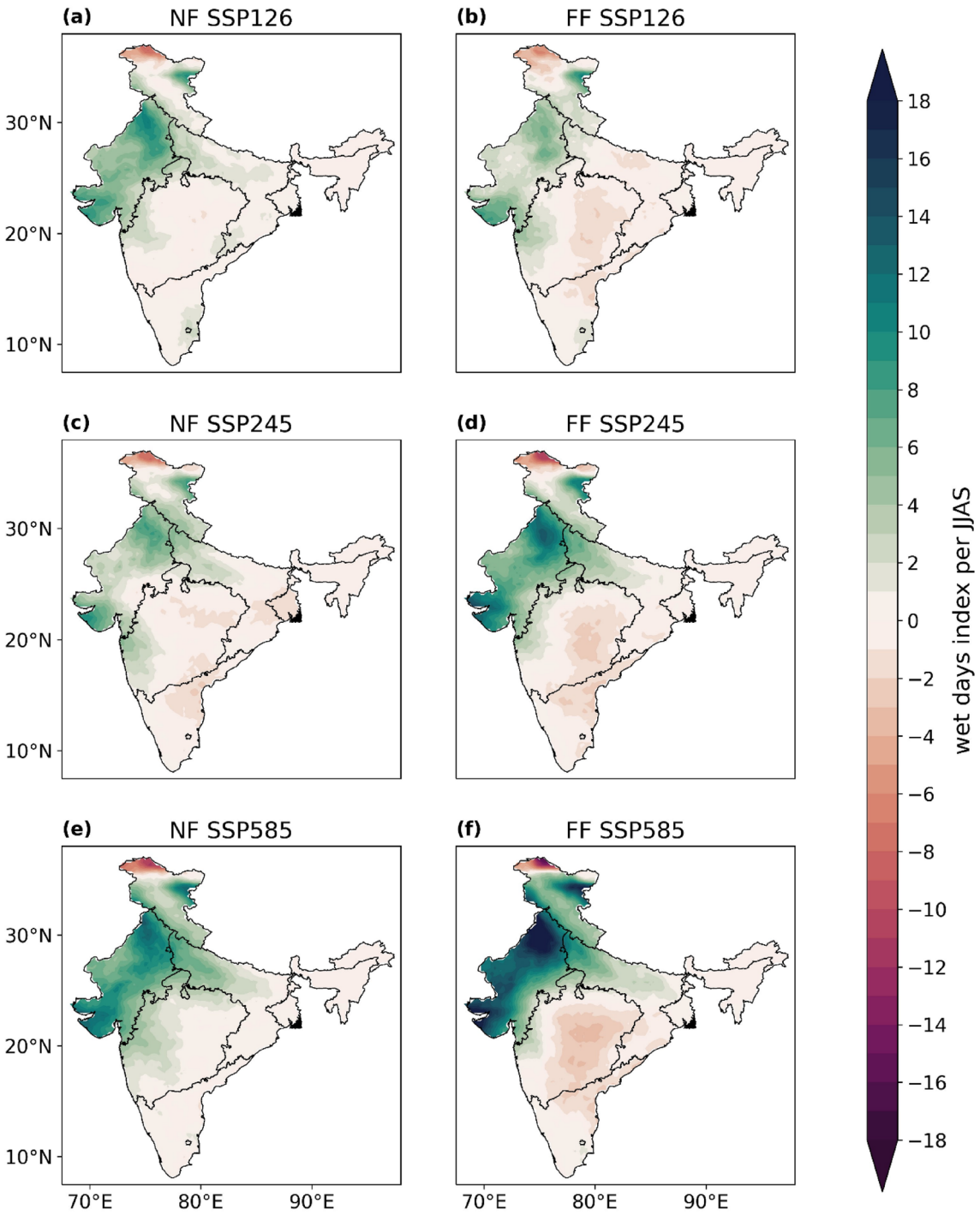

Fig. 14 Wet days Index per JJAS season over India. The first column (**a**, **c**, **e**) shows the NF and the second column (**b**, **d**, **f**) shows the FF for SSP126 (**a**, **b**), SSP245 (**c**, **d**) and SSP585 (**e**, **f**)

- Extreme precipitation has also been shown to increase most dramatically under SSP5-8.5 as well as the VIMT. The most affected regions of India are the PR, WC and NE. The number of wet days will increase over the NW region. This suggests that continued fossil-fuelled development will lead to a more extreme South Asian monsoon approaching the end of the century.
- SSP1.2.6 and SSP2-4.5 increases in precipitation are much less dramatic than SSP5-8.5 meaning that it is possible to lessen the impact given sufficient mitigation strategies are put in place.

Overall, our study suggests that CMIP6 models do show significant improvement in emulating the monsoon precipitation characteristics over homogeneous regions in Indian sub-continent; however, the spatial improvement is inconsistent among the models. As this work only uses CMIP6 models at a low or medium resolution therefore high-resolution dynamical downscaling is needed for a robust decision- and policymaking. In our future work we aim to implement bias corrected high-resolution dynamical downscaling to improve precipitation simulations over India.

Supplementary Information The online version contains supplementary material available at https://doi.org/10.1007/s00382-024-07389-7.

Acknowledgements The authors are thankful to the anonymous reviewers for their useful comments, which help the authors to improve the manuscript. This work was supported by the Research England-Policy Support Fund (PSF)-QR Project C006341.05. We highly appreciate and acknowledge the Climate Research Unit (CRU), ECMWF and the Earth System Grid Federation (ESGF) for making available their precipitation, CMIP6, wind and moisture datasets.

Author contributions Conceptualization and Data Curation: MN, PRT, SD; Analysis and Visualization: MN; Writing: all the authors; Editing: PRT, SD, DK.

Funding PRT acknowledges funding support from Research England-Policy Support Fund (PSF)-QR Project C006341.05.

Data availability The CMIP6 dataset is available at the ESGF data repository (https://esgf-data.dkrz.de/search/cordex-dkrz/. CRU and ERA5 datasets can be downloaded using the link https://crudata.uea.ac.uk/cru/data/hrg/cru_ts_4.05; https://cds.climate.copernicus.eu/cdsapp#!/home/ respectively.

Code availability The codes used in the analysis are available on reasonable request.

Declarations

Conflict of interest Not applicable.

Ethics approval Not applicable.

Consent for publication All the authors gave due consent to collaborate in the study.

References

Almazroui M, Saeed S, Saeed F, Islam M, Ismail M (2020) Projections of precipitation and temperature over the South Asian Countries in CMIP6. Earth Syst Environ 4:297–320. https://doi.org/10.1007/s41748-020-00157-7

Asharaf S, Dobler A, Ahrens B (2012) Soil moisture-precipitation feedback processes in the Indian summer monsoon season. J Hydrometeorol 13:1461–1474. https://doi.org/10.1175/JHM-D-12-06.1

Asharaf S, Ahrens B (2015) Indian summer monsoon rainfall processes in climate change scenarios. J Clim 28:5414–5429. https://doi.org/10.1175/JCLI-D-14-00233.1

Choudhury BA, Rajesh PV, Zahan Y, Goswami BN (2021) Evolution of the Indian summer monsoon rainfall simulations from CMIP3 to CMIP6 models. Clim Dyn 58:2637–2662. https://doi.org/10.1007/s00382-021-06023-0

Dash S, Kulkarni M, Mohanty U, Prasad K (2009) Changes in the characteristics of rain events in India. J Geophys Res 114:D10109. https://doi.org/10.1029/2008JD010572

DeFries R, Mondal P, Singh D, Agrawal I, Fanzo J, Remans R, Wood S (2016) Synergies and trade-offs for sustainable agriculture: nutritional yields and climate-resilience for cereal crops in Central India. Glob Food Sec 11:44–53. https://doi.org/10.1016/j.gfs.2016.07.001

Dutta U, Hazra A, Chaudhari HS, Saha SK, Pokhrel S, Verma U (2022) Unraveling the global teleconnections of Indian summer monsoon clouds: expedition from CMIP5 to CMIP6. Glob Planet Change 215:103873. https://doi.org/10.1016/j.gloplacha.2022.103873

Evans R, Harrison M, Graham R, Mylne K (2000) Joint medium-range ensembles from the Met. Office and ECMWF systems. Mon Weather Rev 128:3104–3127. https://doi.org/10.1175/1520-0493(2000)128%3c3104:JMREFT%3e2.0.CO;2

Eyring V, Bony S, Meehl G, Senior C, Stevens B, Stouffer R, Taylor K (2016) Overview of the Coupled Model Intercomparison Project Phase 6 (CMIP6) experimental design and organization. Geosci Model Dev 9:1937–1958. https://doi.org/10.5194/gmd-9-1937-2016

Falga R, Wang C (2022) The rise of Indian summer monsoon precipitation extremes and its correlation with long-term changes of climate and anthropogenic factors. Sci Rep 12:11985. https://doi.org/10.1038/s41598-022-16240-0

Goswami B (1998) Interannual variations of Indian summer monsoon in a GCM: external conditions versus internal feedbacks. J Clim 11:501–522. https://doi.org/10.1175/1520-0442(1998)011%3c0501:IVOISM%3e2.0.CO;2

Guilbert M, Terray P, Mignot J (2023) Intermodel spread of historical Indian monsoon rainfall change in CMIP6: the role of the tropical pacific mean state. J Clim 36:3937–3953. https://doi.org/10.1175/jcli-d-22-0585.1

Gusain A, Ghosh S, Karmakar S (2020) Added value of CMIP6 over CMIP5 models in simulating Indian summer monsoon rainfall. Atmos Res 232:0169–8095. https://doi.org/10.1016/j.atmosres.2019.104680

IPCC (2014) Climate Change 2014: Synthesis Report. Contribution of Working Groups I, II and III to the Fifth Assessment Report of the Intergovernmental Panel on Climate Change [Core Writing Team, R.K. Pachauri and L.A. Meyer (eds.)]. IPCC, Geneva, Switzerland, 151 pp

IPCC (2022) Climate Change 2022: Mitigation of Climate Change. Contribution of Working Group III to the Sixth Assessment Report of the Intergovernmental Panel on Climate Change [P.R. Shukla, J. Skea, R. Slade, A. Al Khourdajie, R. van Diemen,

D. McCollum, M. Pathak, S. Some, P. Vyas, R. Fradera, M. Belkacemi, A. Hasija, G. Lisboa, S. Luz, J. Malley, (eds.)]. Cambridge University Press, Cambridge, UK and New York, NY, USA. https://doi.org/10.1017/9781009157926

Jiang J, Su H, Wu L, Zhai C, Schiro K (2021) Improvements in cloud and water vapor simulations over the tropical oceans in CMIP6 compared to CMIP5. Earth Sp Sci 8:e2020EA001520. https://doi.org/10.1029/2020EA001520

Katzenberger A, Schewe J, Pongratz J, Levermann A (2021) Robust increase of Indian monsoon rainfall and its variability under future warming in CMIP6 models. Earth Syst Dyn 12:367–386. https://doi.org/10.5194/esd-12-367-2021

Kitoh A, Endo H, Krishna Kumar K, Cavalcanti I, Goswami P, Zhou T (2013) Monsoons in a changing world: a regional perspective in a global context. J Geophys Res Atmos 118:3053–3065. https://doi.org/10.1002/jgrd.50258

Kripalani RH, Kulkarni A, Sabade SS et al (2003) Indian monsoon variability in a global warming scenario. Nat Hazards 29:189–206. https://doi.org/10.1023/A:1023695326825

Krishna Kumar K, Rupa Kumar K, Ashrit R, Deshpande N, Hansen J (2004) Climate impacts on Indian agriculture. Int J Climatol 24:1375–1393. https://doi.org/10.1002/joc.1081

Lau W, Wu H, Kim K (2013) A canonical response of precipitation characteristics to global warming from CMIP5 models. Geophys Res Lett 40:3163–3169. https://doi.org/10.1002/grl.50420

Lun Y, Liu L, Cheng L, Li X, Li H, Xu Z (2021) Assessment of GCMs simulation performance for precipitation and temperature from CMIP5 to CMIP6 over the Tibetan Plateau. Int J Climatol 41:3994–4018. https://doi.org/10.1002/joc.7055

Maharana P, Agnihotri R, Dimri AP (2021) Changing Indian monsoon rainfall patterns under the recent warming period 2001–2018. Clim Dyn. https://doi.org/10.1007/s00382-021-05823-8

Medina S, Houze R, Kumar A, Niyogi D (2010) Summer monsoon convection in the Himalayan region: terrain and land cover effects. Q J R Meteorol Soc 136:593–616. https://doi.org/10.1002/qj.601

Menon A, Levermann A, Schewe J, Lehmann J, Frieler K (2013) Consistent increase in Indian monsoon rainfall and its variability across CMIP-5 models. Earth Syst Dyn 4:287–300. https://doi.org/10.5194/esd-4-287-2013

Moss R, Edmonds J, Hibbard K, Manning M, Rose S, van Vuuren D, Carter T, Emori S, Kainuma M, Kram T, Meehl G, Mitchell J, Nakicenovic N, Riahi K, Smith S, Stouffer R, Thomson A, Weyant J, Wilbanks T (2010) The next generation of scenarios for climate change research and assessment. Nature 463:747–756 https://doi.org/10.1038/nature08823

Mujumdar M, Preethi B, Sabin TP, Ashok K, Saeed S, Pai DS, Krishnan R (2012) The Asian summer monsoon response to the La Nina event of 2010. Meteorol Appl 19(2):216–225

Panda SK, Dash SK, Bhaskaran B, Pattnayak KC (2016) Investigation of the snow-monsoon relationship in a warming atmosphere using Hadley Centre climate model. Glob Planet Change 147:125–136. https://doi.org/10.1016/j.gloplacha.2016.10.013

Pattnayak KC, Panda SK, Saraswat V, Dash N (2018) Assessment of two versions of regional climate model in simulating the Indian Summer Monsoon over South Asia CORDEX domain. Clim Dyn 50:3049–3061. https://doi.org/10.1007/s00382-017-3792-9

Rasmusson E, Carpenter T (1983) The relationship between eastern equatorial pacific sea surface temperatures and rainfall over India and Sri Lanka. Mon Weather Rev 111:517–528. https://doi.org/10.1175/1520-0493(1983)111%3c0517:TRBEEP%3e2.0.CO;2

Ratna SB, Cherchi A, Osborn TJ, Joshi M, Uppara U (2021) The extreme positive Indian Ocean dipole of 2019 and associated Indian summer monsoon rainfall response. Geophys Res Lett 48:e2020GL091497. https://doi.org/10.1029/2020GL091497

Riahi K, van Vuuren D, Kriegler E, Edmonds J, O'Neill B, Fujimori S, Bauer N, Calvin K, Dellink R, Fricko O, Lutz W, Popp A, Cuaresma J, Leimbach M, Jiang L, Kram T, Rao S, Emmerling J, Ebi K, Hasegawa T, Havlik P, Humpenöder F, Da Silva L, Smith S, Stehfest E, Bosetti V, Eom J, Gernaat D, Masui T, Rogelj J, Strefler J, Drouet L, Krey V, Luderer G, Harmsen M, Takahashi K, Baumstark L, Doelman J, Kainuma M, Klimont Z, Marangoni G, Lotze-Campen H, Obersteiner M, Tabeau A, Tavoni M (2017) The Shared Socioeconomic Pathways and their energy, land use, and greenhouse gas emissions implications: an overview. Glob Environ Change 42:153–168. https://doi.org/10.1016/j.gloenvcha.2016.05.009

Schulzweida U, Kornblueh L, Quast R (2021) CDO user's guide. Clim. data Oper Version 2.0.5

Schulzweida, Uwe (2021) CDO User Guide (Version 2.0.0). Zenodo. https://doi.org/10.5281/zenodo.5614769

Sharmila S, Joseph S, Sahai A, Abhilash S, Chattopadhyay R (2015) Future projection of Indian summer monsoon variability under climate change scenario: an assessment from CMIP5 climate models. Glob Planet Change 124:62–78. https://doi.org/10.1016/j.gloplacha.2014.11.004

Sinha PC, Mohanty UC, Kar SC, Kumari S (2013) Role of the Himalayan orography in simulation of the Indian summer monsoon using RegCM3. Pure Appl Geophys 171:1385–1407. https://doi.org/10.1007/s00024-013-0675-9

Song JH, Kang HS, Byun YH, Hong SY (2009) Effects of the Tibetan Plateau on the Asian summer monsoon: a numerical case study using a regional climate model. Int J Climatol 30:743–759. https://doi.org/10.1002/joc.1906

Tiwari PR, Kar SC, Mohanty UC, Dey S, Sinha PC, Shekhar MS (2017) Sensitivity of the Himalayan orography representation in simulation of winter precipitation using Regional Climate Model (RegCM) nested in a GCM. Clim Dyn 49:4157–4170. https://doi.org/10.1007/s00382-017-3567-3

Turner A (2022) Royal meteorological society. [online] RMetS. https://www.rmets.org/resource/indian-monsoon-changing-climate. Accessed 9 Aug 2022

Wang B, Liu J, Kim H, Webster P, Yim S, Xiang B (2013) Northern Hemisphere summer monsoon intensified by mega-El Niño/southern oscillation and Atlantic multidecadal oscillation. Proc Natl Acad Sci 110:5347–5352. https://doi.org/10.1073/pnas.1219405110

Webster P, Magaña V, Palmer T, Shukla J, Tomas R, Yanai M, Yasunari T (1998) Monsoons: processes, predictability, and the prospects for prediction. J Geophys Res Oceans 103:14451–14510. https://doi.org/10.1029/97JC02719

Webster P, Moore A, Loschnigg J, Leben R (1999) Coupled ocean–atmosphere dynamics in the Indian ocean during 1997–98. Nature 401:356–360. https://doi.org/10.1038/43848

Wilks DS (2011) Statistical methods in the atmospheric sciences. Academic Press, Waltham

Yang X, Huang P (2021) Restored relationship between ENSO and Indian summer monsoon rainfall around 1999/2000. The Innovation 2:2666–6758. https://doi.org/10.1016/j.xinn.2021.100102

Yu H, Zhou T, He L (2024) Indian summer monsoon precipitation dominates the reproduction of Circum-global teleconnection pattern: a comparison of CMIP5 and CMIP6 models. J Clim. https://doi.org/10.1175/JCLI-D-23-0644.1

Zhou T, Zhang L, Li H (2008) Changes in global land monsoon area and total rainfall accumulation over the last half century. Geophys Res Lett 35:L16707. https://doi.org/10.1029/2008GL034881

Zhou T, Turner A, Kinter J, Wang B, Qian Y, Chen X, Wu B, Liu B, Zou L, He B (2016) GMMIP (v1.0) contribution to CMIP6: global monsoons model inter-comparison project. Geosci Model Dev 9:3589–3604. https://doi.org/10.5194/gmd-9-3589-2016